A mathematical approach of fuel efficiency for vehicles equipped with Diesel engines

Douglas Marini Albelo
Dr. Fuad Kassab Junior
Dr. Armando Antonio Maria Laganá
Universidade de São Paulo

Abstract

In the last years, the effort spent by automotive companies to deliver a most profitable product to their customers and that preserves the environment has proved the importance of exploiting new methods for maximizing the vehicle fuel efficiency.

Besides the implementation of new technologies such as hybrid electric vehicles (HEVs), fuel cell vehicles (FCVs) and electric vehicles (EVs), several driver assistance systems were developed by automotive companies in the last decades with the aim of improving the fuel efficiency of vehicles equipped with internal combustion engines.

One of the main factors that affects the vehicle fuel efficiency is the way that it is driven, mainly for vehicles equipped with manual transmission, where besides the engine torque control the driver is also responsible for shifting gears. Hence, the development of new technologies that make the operation of this type of vehicle more efficient have proved to be extremely relevant for the automotive Brazilian industry, mainly for commercial vehicles, where alternative measures as drivers training have not achieved the expected results due to the high turnover of these professionals in the Brazilian market.

The purpose of this study is to share a fuel efficiency analysis of commercial vehicles equipped with Diesel engines during positive acceleration phase and also for two hypothetical urban sections travelled with different driving strategies. This analysis aims to provide information that could be used as basis for the development of new active assistance systems to improve the vehicle fuel efficiency.

The mentioned analysis were performed via simulation using MATLAB/Simulink through the non-linear math model that explains the vehicle longitudinal dynamics, as well as a math model designed by the author based on experimental data to explain mathematically the vehicle fuel efficiency.

Keywords: Fuel efficiency, longitudinal vehicle dynamics, energy conservation, mathematical models, fuel economy.

Introduction

Commercial vehicles companies all around the world are working hard on developing new fuel saving strategies as well as reducing pollutant emission by creating new technologies in order to attend government emissions regulations. It is well known that human beings are consuming more natural resources than Earth can provide, therefore fuel saving can only bring advantages for the world. According to the Geneva Environment Network publication in July 2021, the humanity's Ecological Footprint is equivalent to 1.7 Earths [1], where the carbon, the most consumed component, is being consumed faster than any other Footprint component. In 2021, it was responsible for 61% of the total world's Ecological Footprint, which is a significant increase since 1961 [2]. The carbon footprint is associated with the greenhouse gas emissions, where the CO_2 is the most emitted component to the atmosphere with 74,4% of the total GHG emissions, followed by CH_4 with about 17%, according to the CAIT data source from 2018 [3]. The figure 1 presents the global historical GHG emissions from 1990 to 2018. As can be seen, the emission of CO_2 has been increasing year by year, while the emissions of the others GHG as CH_4, N_2O and F_{GAS} have remained more stable since the first measures in 1990.

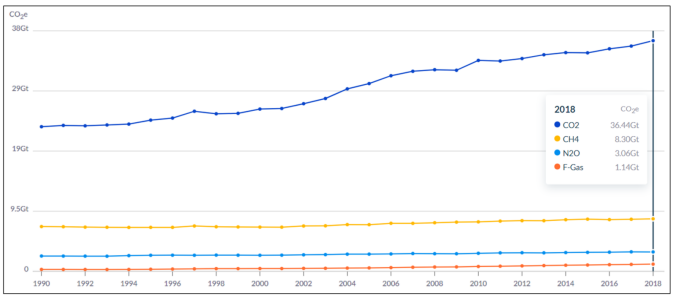

Figure 1: Global historical GHG emissions by gases

Figure 2 shows that the energy sector, which is composed for subsectors as electricity, transportation, manufacture and others, is the main responsible for the total amount of CO_2e emitted in the world followed by the agriculture and industrial process with 76%, 11,9% and 5,9%, respectively.

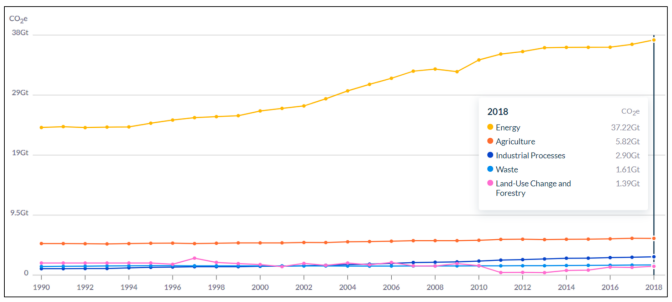

Figure 2: Global historical GHG emissions by sectors

Figure 3 details the global historical GHG emissions of the energy sub-sectors. As can be seen, the main energy sub-sector responsible for the global GHG emissions in 2018 was the electricity/heat followed by transportation and manufacturing/construction with 41,9%, 22.2% and 16,5%, respectively.

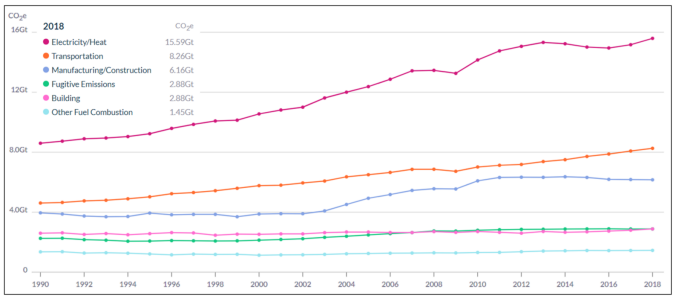

Figure 3: Global historical GHG emissions by energy sub-sectors

It is important to mention that among different types of transportation, the road transportation occupies about 75% of the total amount of the CO_2e emitted by this sub-sector in the world [4].

According to SEEG, Brazil has emitted about 2,2 billions of tons of GHG emissions in 2019, where the land-use change sector is the largest emitter with 44% of the total emissions. The second largest CO_2e emitter is the agricultural sector with 28% followed by the energy sector with 19% [5].

The figure 4 presents the Brazilian historical GHG emission in Mt of CO_2e from 1990 to 2019 as well as the compound annual growth rate, represented by its Brazilian abbreviation TCAC.

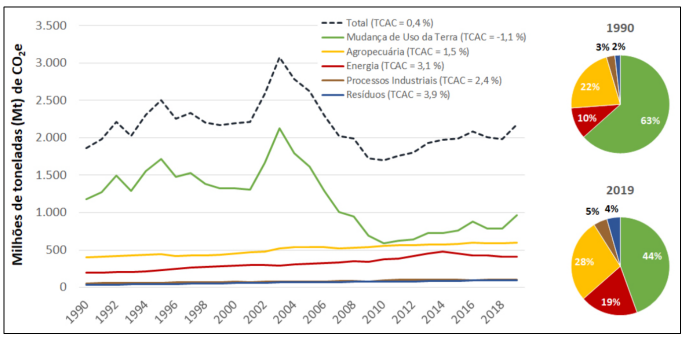

Figure 4: Brazilian historical GHG emissions by sectors

In the Brazilian energy sector, the transportation sub-sector was always the most CO_2e emitter in history, as shown on figure 5. This sub-sector was responsible for emitting 196,5 Mt of CO_2e in 2019 [5]. It represents 8,9% of the total amount of GHG emissions emitted by the country in 2019.

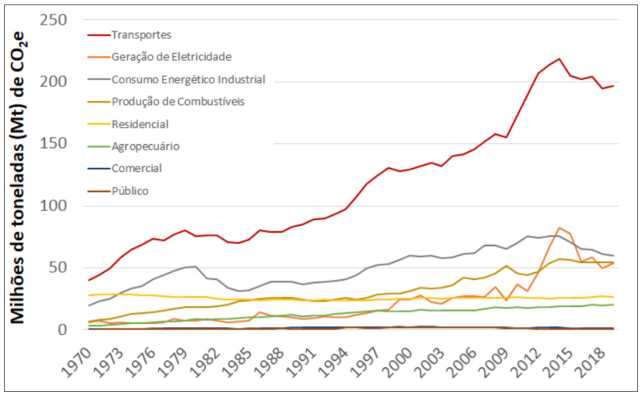

Figure 5: Brazilian historical GHG emissions by energy sub-sectors

The figure 6 presents the equivalent petrol consumption in Mt for the different types of fuels used by the Brazilian transportation sub-sector, it can be seen that Diesel fuel is the most petrol consumer in the country.

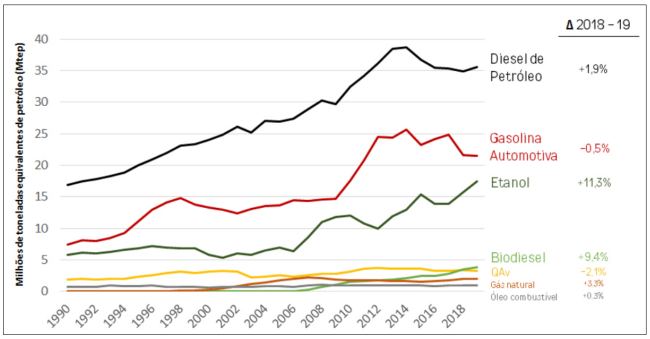

Figure 6: Brazilian fuel consumption history data

In Brazil, this type of fuel is mostly consumed by commercial vehicles as buses, trucks and vans, which are responsible for more than 50% of the total amount of CO_2e emitted in the country as shown on figure 7.

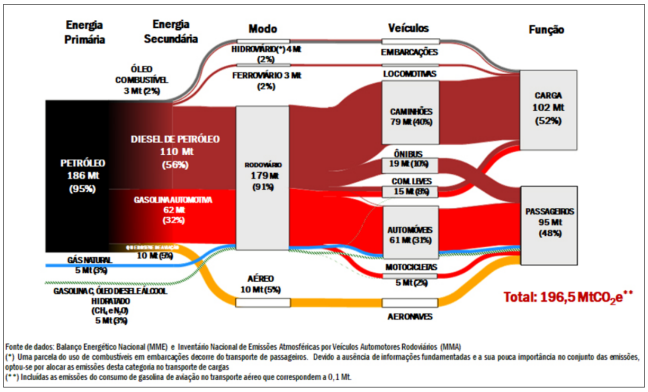

Figure 7: Brazilian GHG emmision in the transportation sector

In addition to the environmental reasons, fuel saving technologies can bring competitive advantages for the companies. The automotive sector is struggling to develop and deliver the most profitable product to their customers. In the Brazilian commercial vehicle market, fuel efficiency is one of the key decision factors that attract owners of commercial vehicle fleets to acquire a certain vehicle branch or type. This importance is growing up year-by-year due to the current high petrol Diesel prices in Brazil.

In the last years, a significant fuel saving was achieved by hybrid electric vehicles (HEVs), fuel cell vehicles (FCVs) and electric vehicles (EVs) technologies.

Once the fuel consumption is highly related to the way a vehicle is driven, several driver assistance methods focused on improvements of gear shifting strategy have also been developed for internal combustion engines.

Driver assistance system can be divided in two groups, passive driver-assistance and active driver-assistance. Passive driver-assistance aims to provide advisor feedback to the driver and it does not have any influence on the vehicle control. On the other hand, active driver-assistance are those where part of the vehicle control is governed by it.

Several methods of active driver-assistance system are currently being applied on vehicles equipped with automatic and automated transmissions, which have brought a significant fuel saving for this type of vehicle. Some of those methods use predictive road gradient information, which aims to support the powertrain controller to define the best vehicle dynamics strategy for the region where the vehicle is being operated. However, it is rare to find active driver assistance systems developed for manual vehicles with the aim of improving fuel consumption.

Some of the newest commercial vehicles equipped with manual transmission have in their feature's portfolio a passive driver-assistance system, which provides gear shifting recommendation signal through the instrument cluster display, in order to support the driver to operate this type of vehicle in a more efficient manner. There are also new technologies implemented for manual vehicles which aims to present grades to the driver via instrument cluster display about how well the driver is operating the vehicle in terms of fuel saving. Although, it can be easily ignored by the driver.

It is difficult to classify the driver behavior, however it is known that drivers can be responsible for as much as 35% variation in fuel consumption [6]. This fuel consumption variation can be easily noticed in urban vehicles with manual transmissions, where the way the vehicle is operated can vary widely among different types of drivers.

Many researchers have presented different methods for improving the vehicle fuel consumption as well as demonstrated how the driving behavior and a gear shifting strategy can affect the vehicle fuel consumption.

The article [7] is one of the mentioned researches, and it has approached the problem of fuel efficiency driving as a problem of numerical optimization. The author has presented a comparison among three different strategies of engine torque control during bus acceleration for three different road slopes. The engine torque control were defined by applying the Pontryagin Minimum´s Principle in order to find the optimal vehicle acceleration path that minimizes the fuel consumption and traveled time. The optimal fuel saving and time strategies were also compared with a 'slow vehicle acceleration rule' strategy.

In [6], a mixed of passive and active driver assistance systems are designed. The authors have utilized nearly 600.000 miles of driving data to identify driving behaviors as well as data based on V2V, V2l, radar, GPS, 3D topography map and the general sensor data acquired from the sensors installed at the vehicle to assist the driver in driving more efficiently. The control system was simulated and validated in one specific scenario where the engine torque demand was adjusted based on the road gradient and to keep a certain vehicle velocity range.

In [8], a controller focused on fuel economy and taking into account travel time duration is developed by adapting the cruising vehicle velocity set-point and schedules gear shifts based on the road gradient. For downhill conditions, the implemented control system opens the drive-line in order to increase its fuel efficiency by letting the vehicle rolling down, similarly with the strategy presented in [6].

Longitudinal vehicle dynamics model

According to [9] and [10], the longitudinal vehicle dynamics can be simply described by

$$F_a = \lambda(n) m \frac{dv(t)}{dt} = F_{tr} - F_{res} \tag{1}$$

where m is the vehicle equivalent mass, $\lambda(n)$ is the inertia of the powertrain rotating parts in terms of gear n, F_a is the vehicle acceleration force, F_{tr} is the vehicle traction force, F_{res} is the total resistance against the vehicle movement and $v(t)$ represents the vehicle speed.

The driving force F_{tr} can be written as follows:

$$F_{tr} = u(t)\eta T_{max}(\omega)\frac{i_{gear}(n) i_{axle}}{r_{wheel}} \tag{2}$$

where $u(t)$ is the control signal ($0 \leq u(t) \leq 1$) that defines the engine torque demand based on the maximum engine torque T_{max}, which depends on engine speed ω, i_{gear} is the gear ratio, which is dependent on the gear engaged n, i_{axle} is the axle ratio, r_{wheel} is the wheel radius and η represents the powertrain efficiency.

The total resistance against the vehicle movement F_{res} can be written by the sum of the following resistance efforts: Rolling friction F_{roll}, aerodynamic drag F_{aero} and gravity F_{grad}.

$$F_{res} = F_{roll} + F_{aero} + F_{grad} \tag{3}$$

In a more detailed manner, F_{res} can be written as follows:

$$F_{res} = mgC_r \cos(\theta) sgn(v(t)) + \frac{1}{2}\rho C_v A v(t)^2 + mg\sin(\theta) \tag{4}$$

where g is the gravity acceleration, C_r is the friction constant, θ is the road gradient, ρ is the air density, C_v is the drag coefficient and A is the vehicle frontal area.

The following differential equation is the result of the combination among equations 1, 2 and 4:

$$\begin{aligned}\dot{v}(t) = \frac{\eta\alpha(n)u(t)T_{max}(\omega)}{m\lambda(n)} - \frac{gC_r\cos(\theta)sgn(v(t))}{\lambda(n)} \\ - \frac{\frac{1}{2}\rho C_v A v(t)^2}{m\lambda(n)} - \frac{g\sin(\theta)}{\lambda(n)}\end{aligned} \tag{5}$$

where $\alpha(n)$ and ω are given by

$$\alpha(n) = \frac{i_{gear}(n) i_{axle}}{r_{wheel}} \tag{6}$$

$$\omega = \alpha_n v(t) \tag{7}$$

Considering a maximum variation of the road gradient between -20% to +20%, equation 5 can be confidently approximated to the equation 8:

$$\dot{v}(t) = \frac{\eta\alpha(n)u(t)T_{max}(\omega)}{m\lambda(n)} - \frac{gC_r sgn(v(t))}{\lambda(n)} - \frac{\frac{1}{2}\rho C_v A v^2(t)}{m\lambda(n)} - \frac{g\theta(t)}{\lambda(n)} \quad (8)$$

where the following approximation was considered:

$$sin(\theta) \approx \theta \quad (9)$$

$$cos(\theta) \approx 1 - \frac{\theta^2}{2} \approx 1 \quad (10)$$

Figures 8 and 9 aims to demonstrate graphically the approximations described by equations 9 and 10, respectively

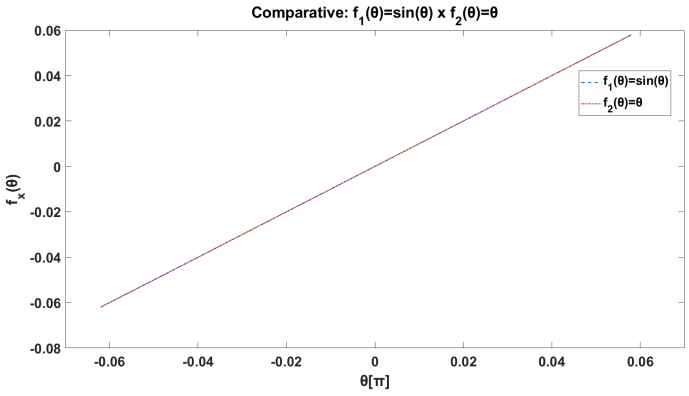

Figure 8: Comparative: $sin(\theta) \times \theta$.

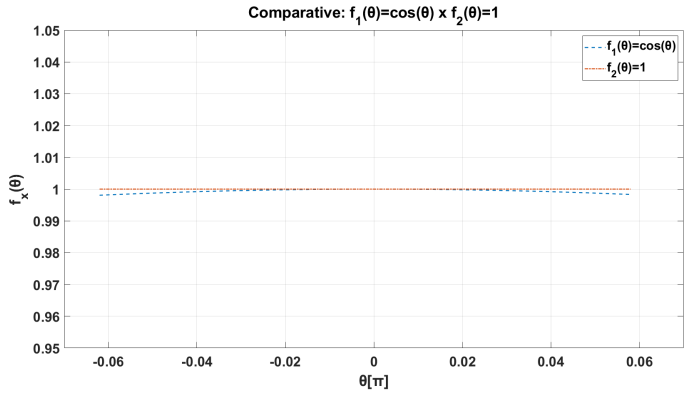

Figure 9: Comparative: $1 \times cos(\theta)$.

Bearing in mind that a road gradient of $\pm$ 20% is equivalent to $\pm$ 11,3°, then, consequently $\pm$ 0,062π.

The term $u(t)T_{max}(\omega)$ from equation 8 can also be replaced by a negative value which represents the braking torque on the engine shaft during a vehicle braking phase.

Fuel efficiency dynamics model

With the aim of explaining the fuel efficiency in terms of the system variables, the following equations were developed by the author based on fuel consumption measurements performed on a real vehicle. As detailed further, the powertrain of the vehicle used in this study is composed by a Diesel four cylinder engine and a manual transmission with six gears combined with a rear tractive axle with final ratio of 4,3.

The first order equation below represents the approximated consumed fuel mass $F_c(T)$ in $[g]$ per each engine revolution $[r]$ in terms of engine torque T with $R^2 = 0,9818$.

$$F_c(T) = 0,0004T \quad (11)$$

By multiplying the equation above by the engine speed in $[r/s]$, the fuel consumption in $[g/s]$ can be described as follows:

$$FC(v(t), u(t), i_{gear}, t) = \frac{v(t)\alpha_n(0,0004u(t)T_{max}(\omega))}{2\pi} \quad (12)$$

Where $\frac{v(t)\alpha_n}{2\pi}$ explains the engine speed in $[r/s]$ and $u(t)T_{max}(\omega)$ the applied engine torque.

It is noted through equation 12 that the fuel consumption in $[g/s]$ varies in terms of engine torque and speed. The fuel consumption in $[g]$ can be explained by integrating $FC(v(t), u(t), i_{gear}, t)$ in terms of time as follows:

$$FC_{eq}(v(t), u(t), i_{gear}), t) = \int_{t_0}^{t} FC(v(t), u(t), i_{gear}), t)dt \quad (13)$$

By dividing the vehicle velocity in $[m/s]$ by equation 12, we can write the vehicle fuel efficiency model in $[m/g]$ (distance travelled per fuel mass) as follows:

$$FE(v(t), u(t), i_{gear}), t) = \frac{v(t)}{FC(v(t), u(t), i_{gear}, t)} \quad (14)$$

By simplifying equation 14, equation 15 can be written:

$$FE(v(t), u(t), i_{gear}), t) = \frac{2\pi}{\alpha_n(0,0004u(t)T_{max}(\omega))} \quad (15)$$

Equation 15 shows that the instantaneous vehicle fuel efficiency is affected by two variables only, α_n and engine torque represented by the term $u(t)T_{max}(\omega)$.

Since i_{axle} and r_{wheel} are constant values on the longitudinal vehicle dynamics model, the variation of α_n depends exclusively on the variation of i_{gear}. Based on that, we can conclude that the instantaneous vehicle fuel efficiency depends on the engine torque $u(t)T_{max}(\omega)$ and gear ratio $i_{gear}(n)$, and as shown by equation 15, the less the values of $i_{gear}(n)$ and $u(t)T_{max}(\omega)$ is, the greater is the instantaneous vehicle fuel efficiency.

The vehicle fuel efficiency average in [m/g] can be written in terms of the travelled time t as follows:

$$FE_a(v(t), u(t), i_{gear}), t) =$$
$$\begin{cases} \int_{t_0}^{t} \frac{1}{t} \frac{2\pi}{\alpha_n(0{,}0004u(t)T_{max}(\omega))} dt, & \text{for } u(t) > 0 \\ \frac{\int_{t_0}^{t} v(t)dt}{FC_{eq}(v(t),u(t),i_{gear}),t)}, & \text{for } u(t) = 0 \end{cases} \quad (16)$$

By matching the instantaneous vehicle fuel efficiency for n and $n+1$, as below:

$$\frac{2\pi}{\alpha_n(0,0004u_n(t)T_{max}(\omega))} = \frac{2\pi}{\alpha_{n+1}(0,0004u_{n+1}(t)T_{max}(\omega))} \quad (17)$$

and simplifying as follows,

$$\frac{i_{gear}(n+1)}{i_{gear}(n)} = \frac{u_n(t)T_{max}(\omega)}{u_{n+1}(t)T_{max}(\omega)} \quad (18)$$

it is possible to show the conditions where the instantaneous vehicle fuel efficiency is equal for the different gear ratios n and $n+1$. According to equation 18, the vehicle fuel efficiency is the same for the different gear ratios n and $n+1$, if and only if, the engine torque relation $\frac{u_n(t)T_{max}(\omega)}{u_{n+1}(t)T_{max}(\omega)}$ is equalized on the same proportionality of $\frac{i_{gear}(n+1)}{i_{gear}(n)}$.

Mathematical models validation

The vehicle used for validating the mathematical models described on the previous sections was a BUS equipped with a Diesel four cylinder engine and a manual transmission composed of six gear ratios combined with a rear tractive axle with final ratio of 4,3.

Figure 10 presents the maximum engine torque available in terms of engine speed $T_{max}(\omega)$:

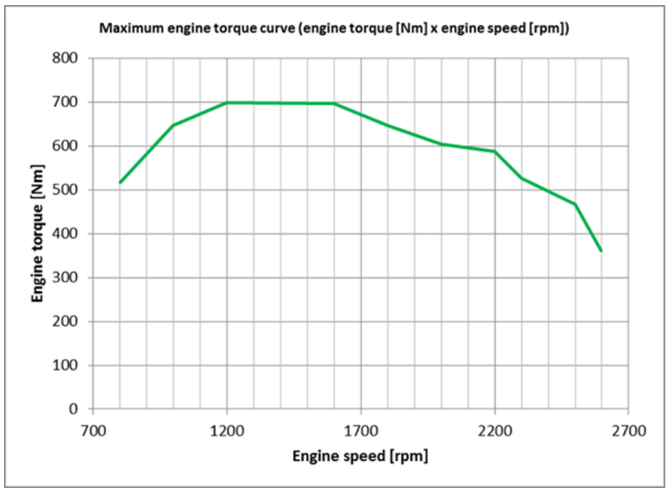

Figure 10: Maximum engine torque in terms of engine speed

Table 1 shows the gear ratio values of the six gears that composes the transmission:

Gear n	Gear ratio i_{gear}	Unit
1	9,201	[-]
2	5,23	[-]
3	3,145	[-]
4	2,034	[-]
5	1,374	[-]
6	1	[-]

Table 1: Gear ratios

Table 2 presents the additional vehicle and powertrain parameters used to calibrate the longitudinal vehicle dynamics model:

Item	Value	Unit
i_{axle}	4,3	[-]
r_{wheel}	0,491	[m]
m	15000	[kg]
η [n=1 to 5]	0,85	[-]
η [n=6]	0,87	[-]
$\lambda(1)$	1,6	[-]
$\lambda(2)$	1,1	[-]
$\lambda(3)$	1,05	[-]
$\lambda(4)$	1	[-]
$\lambda(5)$	1	[-]
$\lambda(6)$	1	[-]

Table 2: Additional powertrain parameters

The inertia of the powertrain rotating parts for each gear ratio $\lambda(n)$ was defined by the author based on the math model responses during the mathematical model validation phase. The longitudinal vehicle dynamics model described by equation 8 and the fuel consumption models in $[g/r]$, $[g/s]$ and $[g]$ described by equation 11, 12 and 13, respectively, were validated on the route detailed by figure 11:

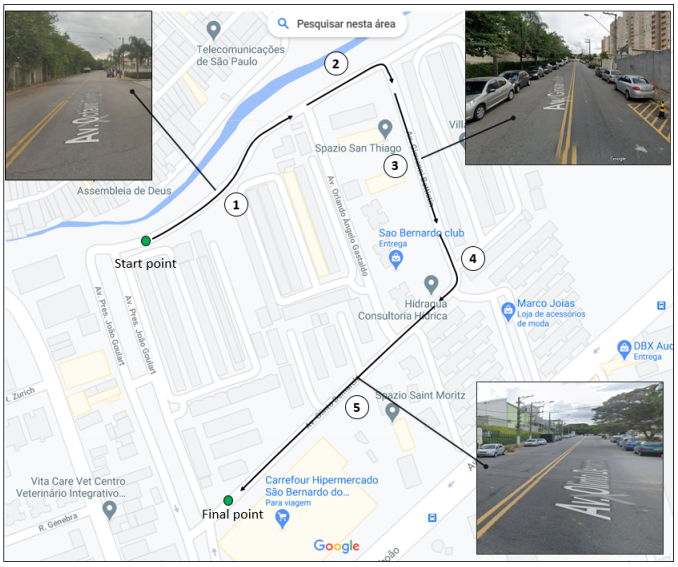

Figure 11: Road used for validating the mathematical models

Figure 12 aims to detail the road slope variation in terms of the main segments of the road. The road gradient was measured with a goniometer along the route and its angle was checked at every five meters. As shown by figure 11 and 12, the road used for validating the math models is composed by a flat road (segment 1), followed by a light decline at the end (segment 2). Next comes a steep hill of approximately 10,5% of road gradient (segment 3), and then, a road gradient of 4,5% (segment 5). The road gradient variation detailed by part 4 connects the

segment 3 with segment 5. In total, this route has approximately 725m of distance.

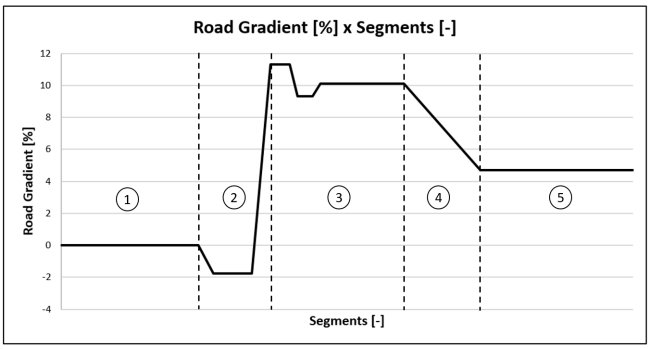

Figure 12: Road gradient along the route

The longitudinal vehicle dynamics model described by equation 8 was calibrated with the vehicle and powertrain data mentioned on figure 10, table 1 and 2. The environmental data as gravity g, friction constant C_r and air density ρ were calibrated with the following values $g = 9,81m/s^2$, $C_r = 0,014[-]$, $\rho = 0,6kg/m^3$. Figure 13 presents a comparative between the maths models responses and the real vehicle data measured along the road detailed by figure 11 and 12. In order to obtain a response from the state variable $v(t)$, the control $u(t)$ multiplied by the instantaneous maximum engine torque $T_{max}(\omega)$ described on equation 8 was supplied with the real engine torque value extracted from the vehicle measurement along the road. The variable θ was supplied manually based on the road gradient detailed on figure 12. The red line is the real vehicle measured data and the black line is the maths models responses.

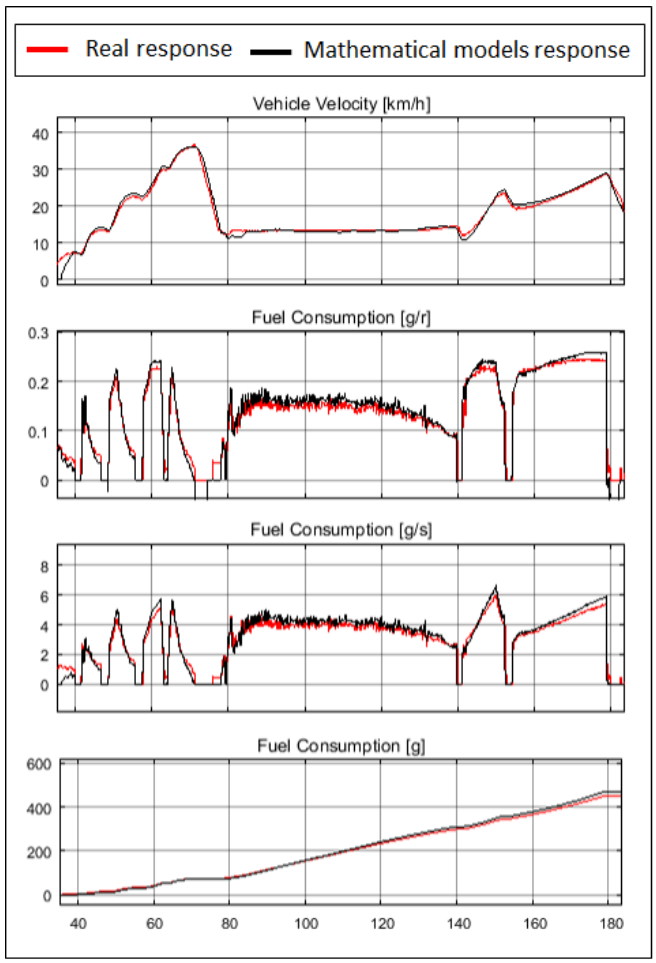

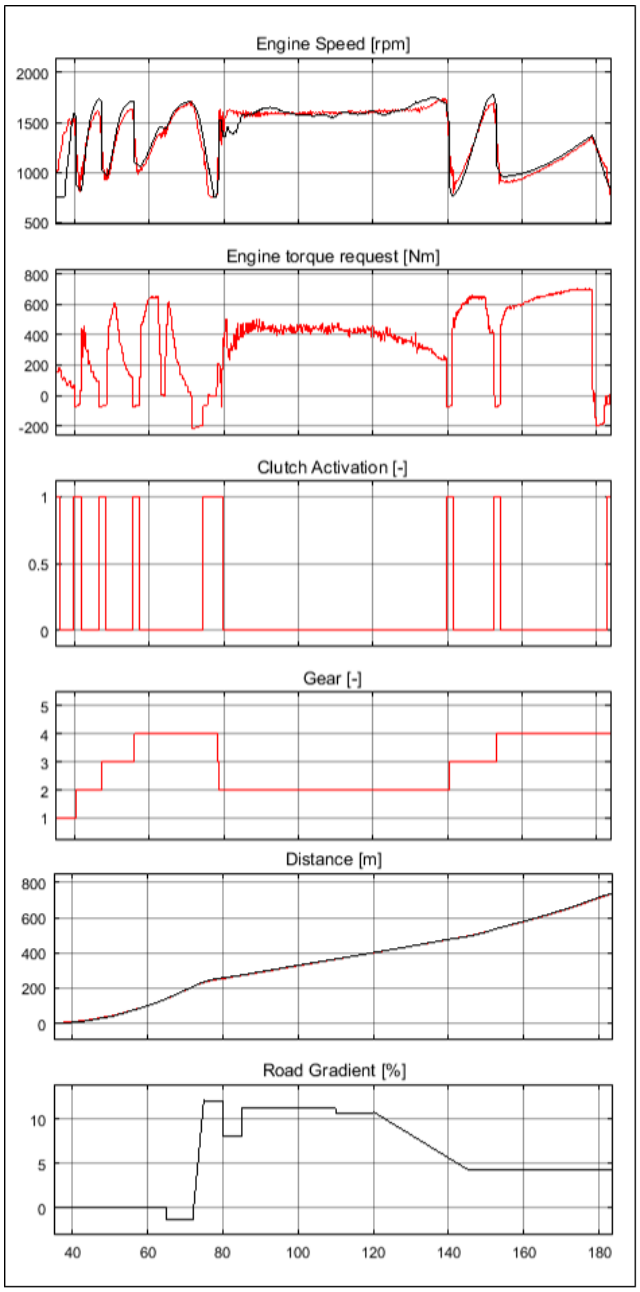

Figure 13: Comparative between math model and real vehicle response

Firstly, we can note that the mathematical models described by equations 8, 11, 12 and 13 have shown a good response when compared with the real vehicle response, however, it is also possible to note some small gaps between them. Those gaps can be explained by some small errors with the calibration of the math model variables as η, $\lambda(n)$, C_r, ρ, C_v, A, m.

Besides the calibration of the math model, the real vehicle has as part of its real dynamical response the lateral forces that acts on the wheels around the curve. This effort is not part of the longitudinal vehicle math model used in this study and this can also generate some gaps that the vehicle math model is not able to reproduce.

Since the road gradient variable θ is one of the math model input, it was defined in a way that the math model variable $v(t)$ gets as much closest as possible of the real vehicle velocity.

Then, some small gaps between the road gradient measured and presented on figure 12 and the road gradient signal shown on figure 13 can

be noted as well.

Fuel efficiency analysis during positive vehicle acceleration

The following analysis was performed using the mathematical models developed and described on the previous sections and aims to demonstrate graphically the vehicle fuel efficiency and fuel consumption in terms of vehicle velocity during positive vehicle acceleration phase for different driving strategies and road slopes.

The dynamic behavior of engine torque, vehicle acceleration, distance travelled, engine speed, gears and travelled time are also presented in terms of vehicle velocity. The analysis was performed for three different road slope conditions, they are: 0%, +5% and -5%.

Figure 14 aims to present a comparison of fuel efficiency and vehicle performance for three different controls and considers the road slope equal 0%. The gears are shifted in sequence from $n = 1$ to $n = 5$ at engine speed close to 1600 rpm and vehicle velocity varying from 1 m/s to 14 m/s.

The blue line and orange line present the math models dynamics for $u_1(t) = 1$ and $u_2(t) = 0,6$, respectively. Both controls are applied for $1 \leq n \leq 5$. The yellow line presents the math model dynamics for $u_3(t) = 0,3$ for $1 \leq n \leq 4$ and $u_3(t) = 0,4$ for $n = 5$. The step from 0.3 to 0.4 on the control signal $u_3(t)$ is due to the fact that the engine torque generated by $u_3(t) = 0,3$ is not able to produce enough driving force for the fifth gear to overcome the total resistance against its movement.

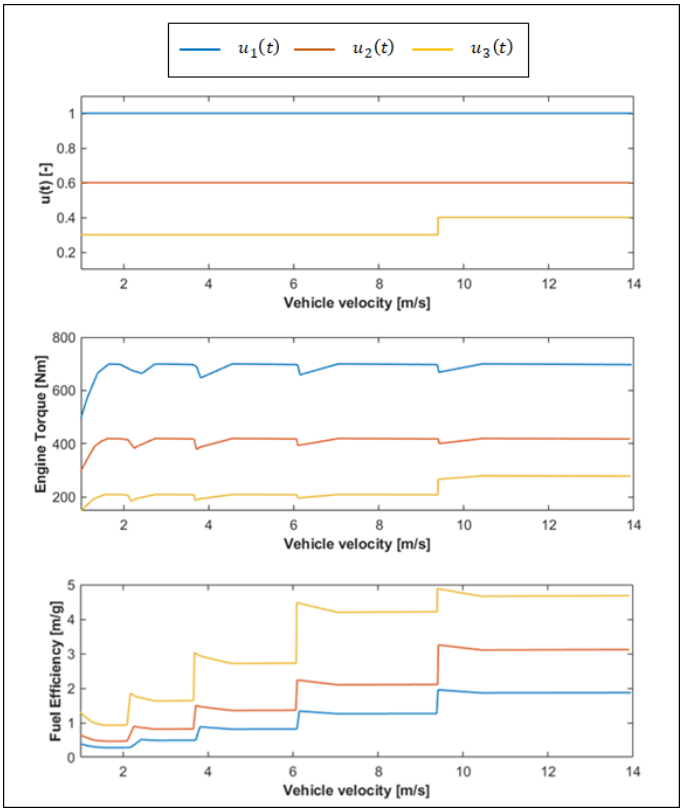

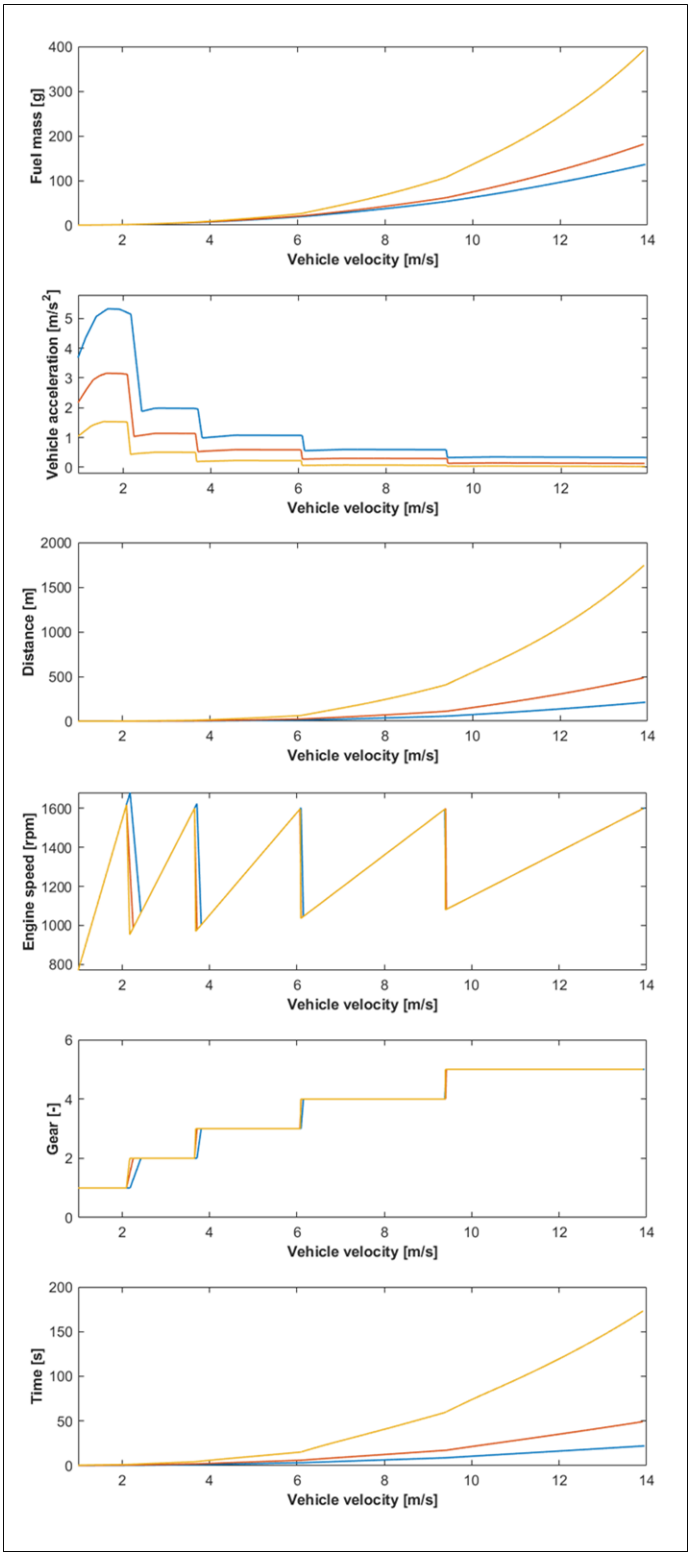

Figure 14: Fuel efficiency analysis for road slope=0%

We can note that the greater the control $u(t)$ is, the less is the consumed fuel mass $FC_{eq}(v(t), u(t), i_{gear}), t)$ during the positive acceleration phase, this meets with the results published on [7] for the same road slope value. On the other hand, we can see that the less the control $u(t)$ is, the greater is the instantaneous fuel efficiency $FE(v(t), u(t), i_{gear}), t)$. This means that the relation between distance travelled and consumed fuel mass is higher when lower engine torque is required. The fuel efficiency topic is not mentioned on [7].

We can also note graphically the direct proportionality between engine torque and vehicle acceleration in terms of vehicle velocity.

Figure 15 aims to present the same comparison for a new road slope of +5% and two different control signals. The gears are shifted in sequence from $n = 1$ to $n = 4$ at engine speed close to 1900 rpm and vehicle velocity varying from 1 m/s to 11.5 m/s.

The blue line presents the math models dynamics for $u_4(t) = 1$ and $1 \leq n \leq 4$, while the orange line considers $u_5(t) = 0,6$ for $1 \leq n \leq 3$ and $u_5(t) = 1$ for $n = 4$, this control step also occurs due to the fact that the engine torque generated by $u_5(t) = 0,6$ is not able to produce enough driving force for $n = 4$ to overcome the total resistance against the vehicle motion.

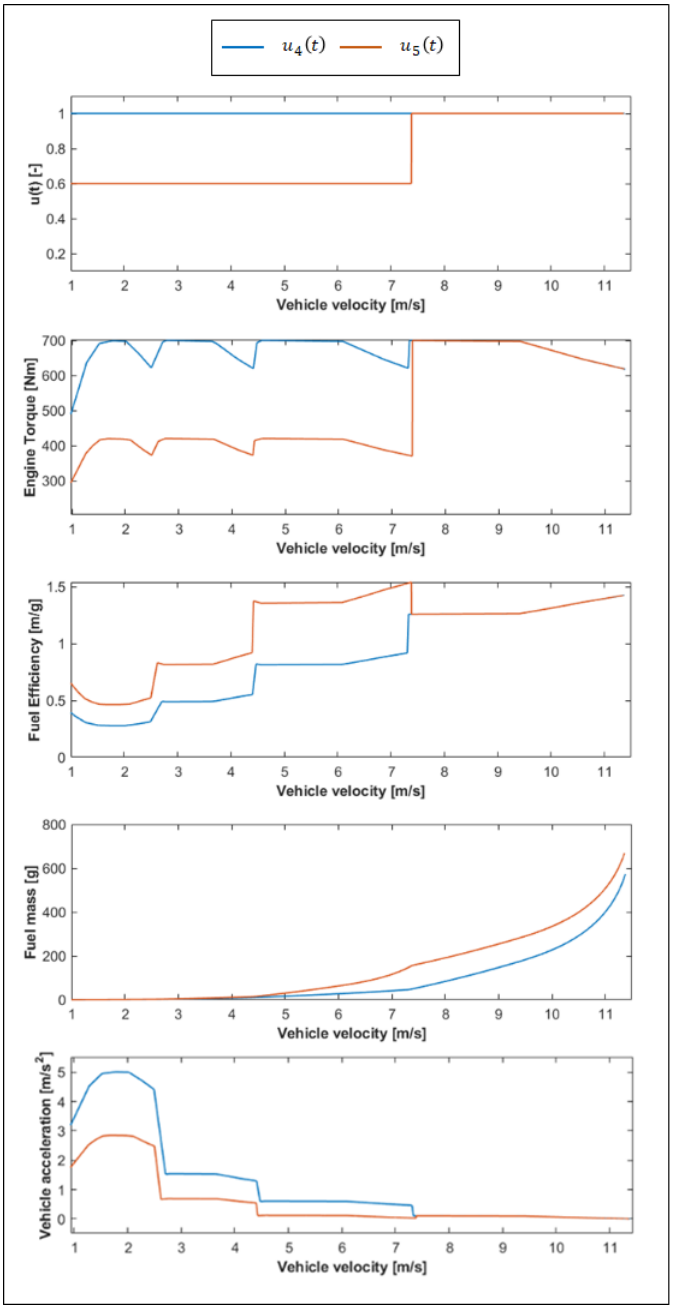

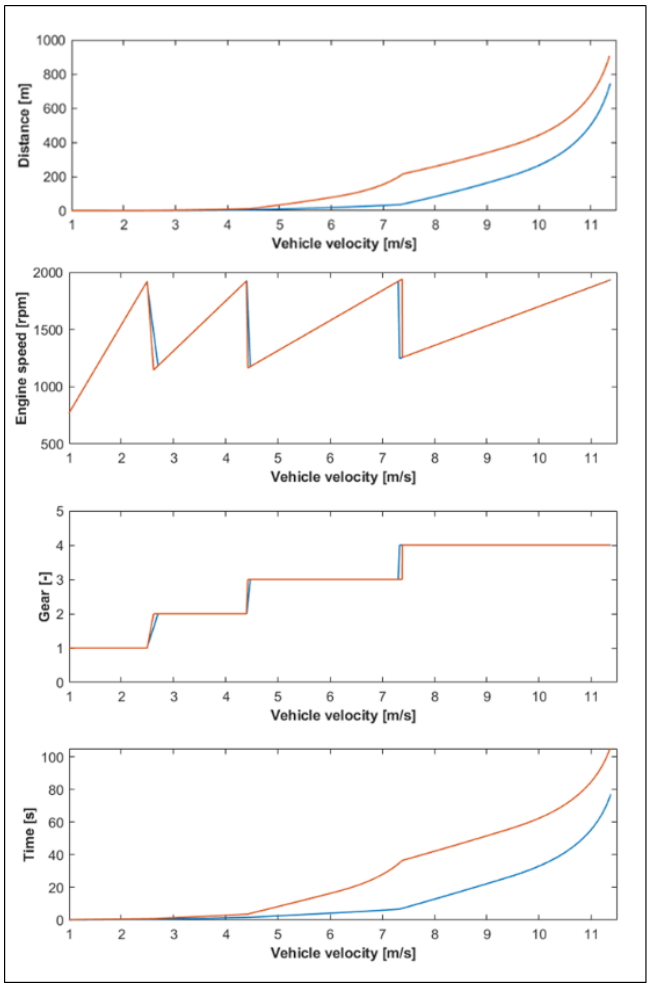

Figure 15: Fuel efficiency analysis for road slope of +5%

The results presented on figure 15 by operating the vehicle through the two different control strategies $u_4(t)$ and $u_5(t)$ are similar to the results presented on figure 14. This means that the greater the control $u(t)$ is, the less is the consumed fuel mass $FC_{eq}(v(t), u(t), i_{gear}), t)$ during the positive vehicle acceleration phase. This also meets with the results published on [7] for the road slope value of +5%. On the other hand, we can also note again that the instantaneous fuel efficiency $FE(v(t), u(t), i_{gear}), t)$ is greater for lower values of $u(t)$.

The figure 16 considers the road slope of -5% and three different control signal $u_6(t)$, $u_7(t)$ and $u_8(t)$. In this simulation, the gears are shifted in sequence from $n = 1$ to $n = 5$ at engine speed around 1550 rpm and vehicle velocity varying from 1 m/s to 13.5 m/s. The blue line presents the math models dynamics for $u_6(t) = 1$, orange line for $u_5(t) = 0,6$ and yellow line for $u_6(t) = 0,3$. The three controls are kept constant during all the positive vehicle acceleration phase.

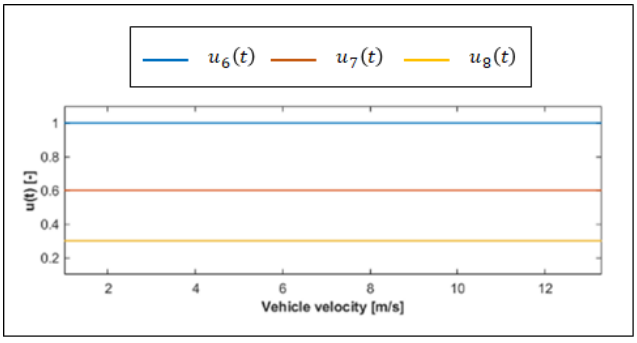

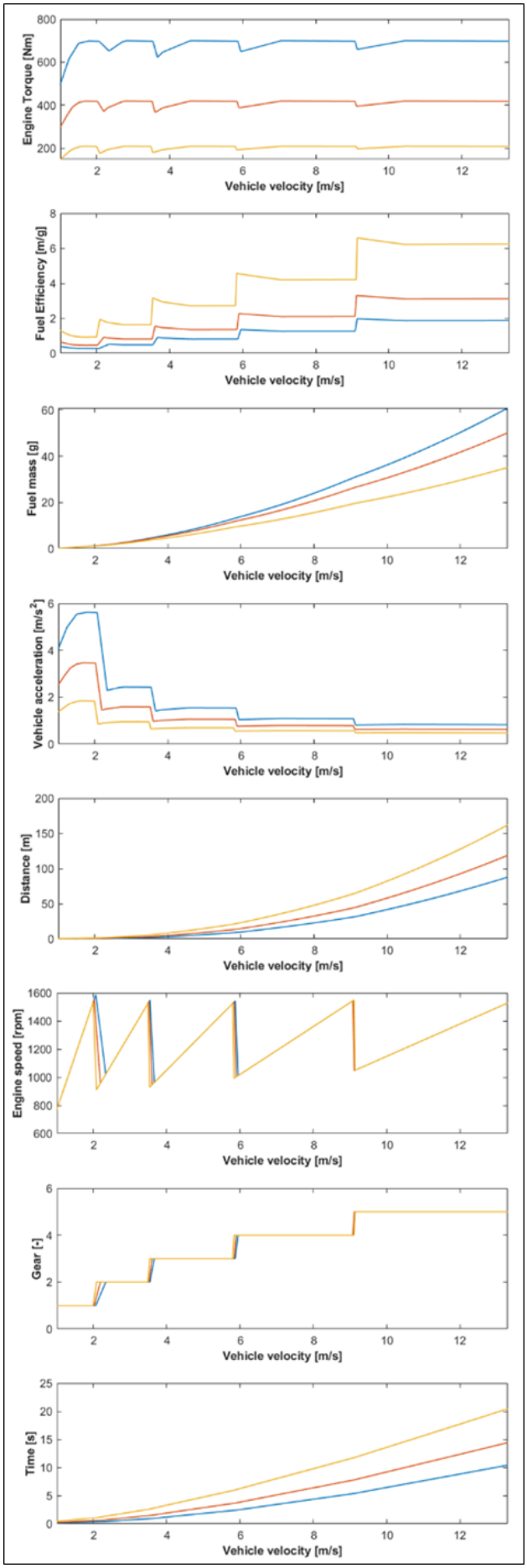

Figure 16: Fuel efficiency analysis for road slope = -5%

The simulation presented on figure 16 shows an opposite behavior of the consumed fuel $FC_{eq}(v(t), u(t), i_{gear}), t)$ when compared with the results obtained previously for the road slopes of 0% and +5% presented on figures 14 and 15, respectively. Here, the controls $u_6(t)$, $u_7(t)$ and $u_8(t)$ are directly proportional with the consumed fuel mass $FC_{eq}(v(t), u(t), i_{gear}), t)$ even during the positive vehicle acceleration phase. This means that the less the control $u(t)$ is, the less is the consumed fuel mass $FC_{eq}(v(t), u(t), i_{gear}), t)$. This also meets with the results published on [7].

With this negative road slope condition, we can note that gravity is producing tractive effort instead of resistance against the vehicle movement and this supports the engine torque to generate positive vehicle acceleration.

The fuel efficiency behavior is kept the same, then, in this new situation where the road slope is negative, its values are greater for lower control values.

Fuel efficiency analysis for two different hypothetical urban road segments and driving strategies

The following simulation aims to present the vehicle performance behavior and efficiency by traveling two different hypothetical urban road segments through different driving strategies.

As shown on figure 17, the first urban segment created by the author is composed by a flat road between $S_0 = 0m$ and $S_2 = 150m$, followed by a decline section with a road slope of -5% between S_2 and $S_4 = 250m$, next comes another flat segment between S_4 and $S_6 = 400m$.

In this simulation the vehicle starts its motion from S_0 and gradually increases its velocity through the two different controls and gear shifting strategies. For the both presented driving strategies, the vehicle must stop at S_2, S_4 and S_6. The points S_1, S_3 and S_4 are the points where the vehicle starts slowing down to reach the designated stopping places S_2, S_4 and S_6 with $v(t) = 0$.

The control $u_1(t)$ takes into account a type of vehicle operation where higher levels of vehicle acceleration are reached and the gear shifting is performed at higher engine speeds. The control $u_2(t)$ takes into account a type of vehicle operation with lower levels of vehicle acceleration when compared with the control strategy $u_1(t)$ and this driving strategy the gears are shifted at lower engine speeds.

The simulation shows that the consumed fuel by travelling the road sections with $u_2(t)$ and by performing gear shifts at lower engine speeds was approximately 87g, while by travelling with $u_1(t)$ and performing gear shifts at higher engine speeds was approximately 250g, 187% higher. Otherwise, the time spent to conclude the route with $u_1(t)$ was 52,5s, while with $u_2(t)$ it took 87,3s, 66% higher.

Another point to emphasize is the braking effort spent to stop the vehicle at S_2, S_4 and S_6. The vehicle deceleration between the sections S_1 to S_2, S_3 to S_4 and S_5 to S_6 is higher when travelled with $u_1(t)$ than with $u_2(t)$.

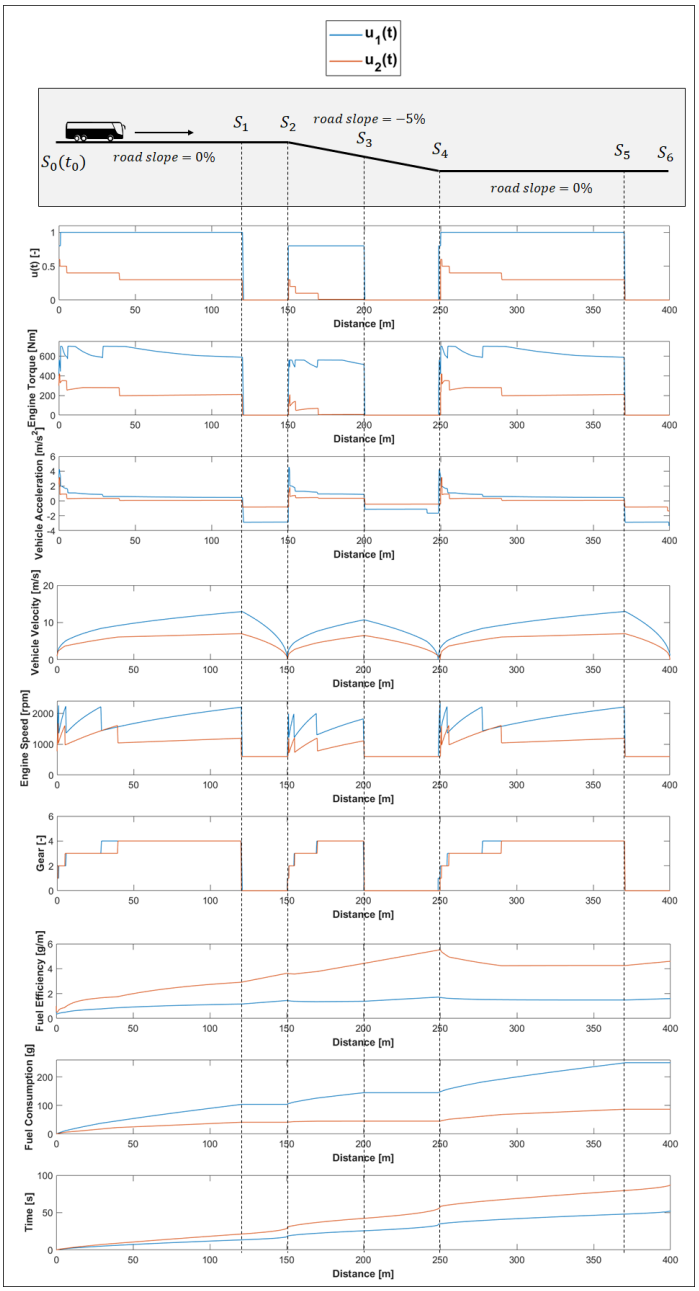

Figure 17: Fuel efficiency analysis

Figure 18 shows the second hypothetical urban segment which has a total distance of 600m. As shown on figure 18, it is composed by a flat road between $S_7 = 0m$ and $S_9 = 200m$, next comes a section with a road slope of +5% between S_9 and $S_{11} = 400m$, and then, another flat segment between S_{11} and $S_{13} = 600m$.

In this simulation the vehicle also starts its motion from S_7 and gradually increases its velocity through the two different controls and gear shifting strategies. Here, the vehicle stopping place are located at S_9, S_{11} and S_{13}. The points S_8, S_{10} and S_{12} are the points where the vehicle starts slowing down to reach the mentioned stopping places with $v(t) = 0$.

As we can see on figure 18, the difference between the two driving strategies is not so high when compared with the driving strategies presented on figure 17. In this new simulation the gaps between the controls $u_3(t)$ and $u_4(t)$ is lower when compared with $u_1(t)$ and $u_2(t)$. However, the control $u_3(t)$ also aims to simulate a type of driver that operates the vehicle with higher levels of vehicle acceleration and shifts gears at higher engine speeds, while the control $u_2(t)$ aims to simulate a type of driver that operates the vehicle with lower levels of acceleration and shifts gears at lower engine speeds.

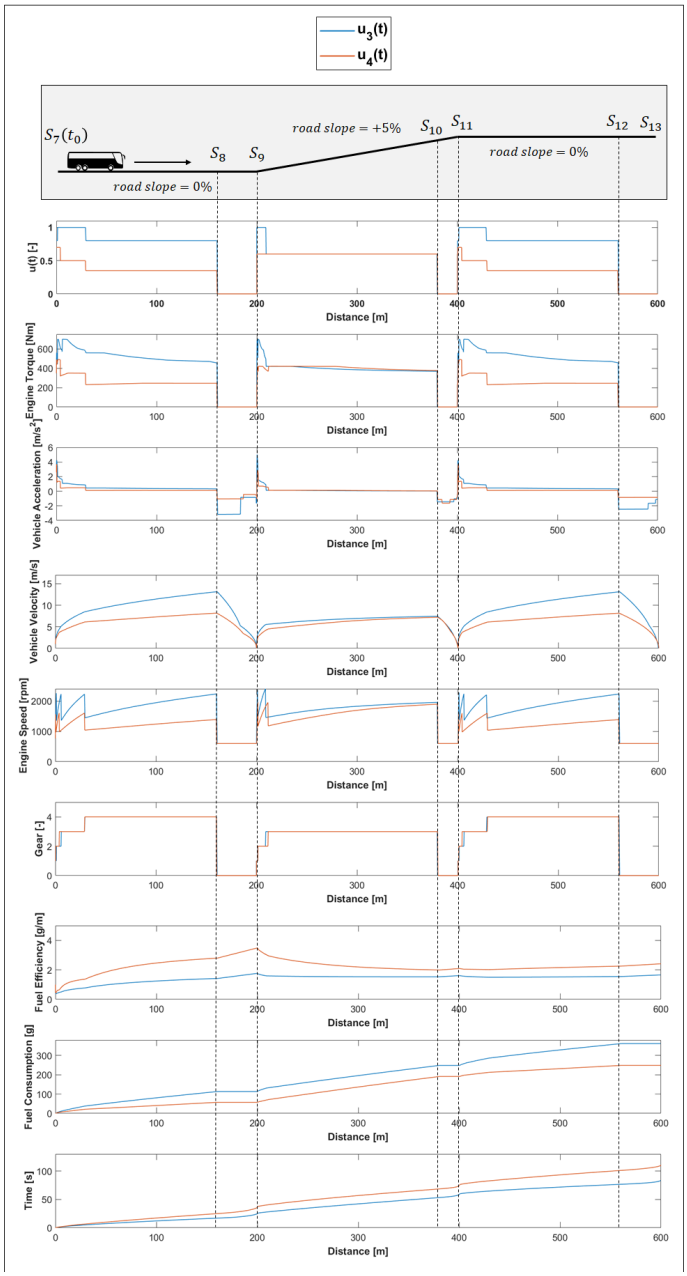

Figure 18: Fuel efficiency analysis

This simulation shows that by travelling this new mentioned road sections using the control $u_4(t)$ and performing gear shifts at lower engine speeds, the consumed fuel mass was 249g, while by travelling the sections with $u_3(t)$ and performing gear shifts at higher engine speeds, the consumed fuel mass was approximately 362g, 45% higher. The time spent to conclude the route with $u_3(t)$ was 84s, while with $u_4(t)$ it took 111s, 32% higher.

As also mentioned in the previous simulation the braking effort spent to stop the vehicle at the mentioned stopping places is higher when travelled with $u_3(t)$ than with $u_4(t)$, due its higher vehicle velocity at the braking points S_8, S_{10} and S_{12}.

Conclusion

The results achieved and presented in this article by simulating the vehicle fuel efficiency during positive vehicle acceleration phases using different driving strategies and also the fuel consumption results by travelling the two hypothetical urban road sections via different driving strategies allow us to conclude that active assistance systems for urban commercial vehicles can be developed in order to force ”bad drivers” to operate the vehicle in a more efficient manner, mainly for commercial urban vehicles equipped with manual transmissions.

The proposed active driver assistance systems can be developed in a way to avoid ”bad drivers” to shift gears at higher engine speeds as well as avoid the vehicle operation with high levels of positive vehicle acceleration, mainly for negative road slopes regions.

In a more detailed manner, the active assistance system should be adjustable in order to attend different vehicles applications and configuration. With the aim of forcing the drivers to perform up-shifting at lower engine speeds, a control system for limiting the maximum engine speed in terms of the road gradient and gears could be developed as well as a control system for limiting the vehicle acceleration in terms of gears.

References

1. Earth Overshoot Day 202. Geneva Enviroment Network, 2021. Available on: https://www.genevaenvironmentnetwork.org/resources/updates/earth-overshoot-day-2021/. Accessed on: February 26th 2022

2. David Lin, Ph.D, Leopold Wambersie MSc, Mathis Wackernagel, Ph.D., Earth Overshoot Day. Global Footprint Network. “Estimating the Date of Earth Overshoot Day 2021”. May 2021

3. Climate Watch. Historical GHG Emissions. Available on: https://www.climatewatchdata.org/ghg-emissions?breakBy=gaschartType=lineregions=WORLDsource=CAIT

4. Mengpin Ge and Johannes Friedrich. 4 gráficos para entender as emissões de gases de efeito estufa por país e por setor. WRI Brasil, 2020. Available on: https://wribrasil.org.br/pt/blog/2020/02/quatro-graficos-explicam-emissoes-de-gases-de-efeito-estufa-por-pais-e-por-setor

5. Felipe Barcellos, pesquisador do IEMA. As emissões brasileiros de gases de efeito estufa nos setores de Energia e de Processos Industriais em 2019. IEMA, 2020. Available on: https://energiaeambiente.org.br/as-emissoes-brasileiras-de-gases-de-efeito-estufa-nos-setores-de-energia-e-de-processos-industriais-em-2019-20201201

6. Rajeev Verma, Nikhil Nahar, Zhijun Tang and Benjamin Saltsman (Eaton Corporation, USA). 2013. “A Driver Assistance System for Improving Commercial Vehicle Fuel Economy”. SAE International. Symposium on International Automotive Techinology, 2013

7. Romano Impero Abenavoli, Maurizio Carlini, Henryk Kormanski and Krystyna Rudzinska. 1999. “Fuel Economy Improvement by Vehicle Control Optimization”. SAE International. 34th Intersociety Energy Conversion Engineering Conference Vancouver, British Columbia August 2-5, 1999

8. D’Amato, A., Donatantonio, F., Arsie, I., and Pianese, C., ”Development of a Cruise Controller Based on Current Road Load Information with Integrated Control of Variable Velocity Set-Point and Gear Shifting,” SAE Technical Paper 2017-01-0089, 2017, doi:10.4271/2017-01-0089.

9. KARL JOHAN ASTRÖN and RICHARD M. MURRAY, Feedback Systems An Introduction for Scientists and Engineers, Princeton University Press, 2009, version V2.10b. Library of Congress Cataloging-in-Publication Data. ISBN-13: 978-0-691-13576-2 (alk. paper) ISBN-10: 0-691-13576-2 (alk. paper) 1. Feedback control systems. I. Murray, Richard M., 1963-. II. Title. TJ216.A78 2008. 629.83–dc22. 2007061033

10. Albelo, D., Dias, R., Neves, R., and Paterlini, B., ”Vehicle Dynamic Control using Vehicle Network Toolbox from MATLAB/Simulink®,” SAE Technical Paper 2021-36-0420, 2022, https://doi.org/10.4271/2021-36-0420.

11. Kirk, D.E. (2004) Optimal Control Theory (An Introduction). Dover Publications, INC. Mineola, New York.

Contact Information

Douglas Marini Albelo, Senior Product Development Engineer at Mercedes-Benz do Brasil, Graduate Student at University of São Paulo (USP).
douglas.albelo@usp.br
douglas_marini.albelo@daimlertruck.com